scientific reports

Check for updates

OPEN

Analysis of time-fractional cancer-tumor immunotherapy model using modified He-Laplace algorithm

Mubashir Qayyum[1], Sidra Nayab[1], Imran Siddique[2,3] & Abdullatif Ghallab[4]✉

Cancer encompasses various diseases characterized by the uncontrolled growth of abnormal cells, which can invade healthy tissues and spread throughout the body, making it the second leading cause of death worldwide. This study presents a fractional cancer treatment model with immunotherapy to enhance understanding of cancer's mathematical framework and behavior. The model comprises fractional differential equations analyzed using the Caputo-fractional derivative, aiming to control cancer growth while considering cell population metrics. A framework integrating various homotopies and Laplace transforms is developed to explore cancer's complexities. Simultaneous solution profiles for effector immune cells and tumor cells illustrate their mutual influence. The model examines parameters such as the death rate of immune cells, natural tumor growth rate, rate of immune cells killing fractional tumor cells and numerous others graphically for clarity. The fractional parameter β is visually represented through 2D, 3D, and contour plots. This comprehensive analysis validates the proposed approach, suggesting its applicability to other complex cancer treatment models for better decision-making in cancer treatment.

Keywords Cancer treatment model, He-Laplace algorithm, Caputo fractional derivative, Immune cells, Tumor cells, Immunotherapy

Cancer, throughout history of mankind has been an ever evolving and fatal disease which has been as much of a matter of concern for humans from the dawn of time as it is in the present day[1,2]. Due to the deadly nature of this disease, researchers, biologists, physicists, chemists and mathematicians all around have been writing and proposing a multitude of methods and approaches to tackle and grasp the reason for the unpredictable nature of this disease so as to outrun it and save lives of millions susceptible individuals[3]. Some of the earliest evidence of cancer is found in fossilized bone tumors, ancient Egyptian mummies, and historical manuscripts[4]. Mummies have shown growths indicative of osteosarcoma, a type of bone cancer. The earliest known description of cancer-though the term "cancer" was found in Egypt and dates back to around 3000 BC. This description is recorded in the Edwin Smith Papyrus, a fragment of an ancient Egyptian textbook on trauma surgery. It details eight cases of breast tumors or ulcers that were treated by cauterization using a tool called the fire drill. The text wrote about the condition, *there is no treatment* which unfortunately, even after thousands of years still holds true[5]. Hippocrates, the famous Greek physicist also knows as 'The Father of Medicine' coined the terms *carcinos* and *carcinoma* to refer to non-ulcerating and ulcerating tumors, respectively.[6] In Greek, these terms refer to a crab, likely applied to the disease due to the resemblance of cancer's finger-like projections to the shape of a crab. The Roman physician, Celsus was the one who later transcribed the Greek word into 'Cancer' which is basically a latin word for crab. Although the sixteenth century researchers and scientists laid down the path for scientific oncology, it was not until the nineteenth century that mankind could finally microscopically analyze the disease and led to researchers being capable of presenting numerous treatment models to cure some kinds of early stage cancers.

Cancer is a broad category of diseases united by a common factor that when normal cells transform into cancerous cells they, proliferate and spread[7]. There are more than hundred kinds of cancers which are divided according to their place of origin in the body and the tissues they affect[8]. However, it is subdivided into three main types, *Solid cancers* i.e carcinoma (that effect epithelial tissues) and sarcoma (that effects connective tissues), *Blood cancers* which form in blood cells and *Mixed cancers* which hybrids two types for example carcinosarcoma.

[1]Department of Sciences and Humanities, National University of Computer and Emerging Sciences, Lahore, Pakistan. [2]Department of Mathematics, University of Sargodha, Sargodha 40100, Pakistan. [3]Mathematics in Applied Sciences and Engineering Research Group, Scientific Research Center, Al-Ayen University, Nasiriyah 64001, Iraq. [4]Department of Computer Science, University of Science and Technology, P.O. Box: 13064, Sana'a, Yemen. ✉email: ghallab@ust.edu.ye

Cancer diagnosis are so common that 1 in 4 people will develop some kind of cancer at some point in their life, which is exactly why cancer research has already been a chief concern for biomedical scientists and with the advent of the notion of mathematics and biology being more closely related than majorly disconnected, many cancer treatment models have been put forward to give a mathematical insight into the matter[9]. The primary goal of immunotherapy is to enhance the body's natural ability to fight a disease by improving the effectiveness of the immune system[10,11]. Unlike traditional treatments like chemotherapy[12] or radiation[13], which directly target cancer cells, immunotherapy aims to enhance or restore the immune system's ability to recognize and destroy cancer cells[14].

The significant role of mathematical modeling and evaluation has given rise to various different kind of tools to manipulate, fight and to an extent control different epidemic outbreaks and infection waves which have spread out[15]. Different authors suggested different kind of cancer models for example, D'Onofrio et al. investigated the role of mathematical modeling in combination therapy for tumors. Kermack and McKendrick[16] highlighted the importance of mathematical modeling in understanding biological events related to epidemics. Few other models have been presented to analyze the behavior of this disease for better prediction and cure[17]. There are many studies on cancer-tumor models in classical and fractional environments. Javeed et al. studied various cancer models by means of curve fittings[18]. Patterson et al. discussed lung cancer with respect to prognostic markers[19]. Qayumm et al. analyzed cancer-tumor with respect to killing rates[17]. Zhang et al.[20] discussed breast cancer in humans and its mathematical consequences. Quaranta et al.[21] simulated tumor models with special reference to treatment and prognosis. Tabassum et al.[22] worked on the growth of cancer-tumor and how the modeling of such complex structure should be made to capture it in its entirety. Pillis et al.[23] discussed a little about immunotherapy treatment and its impact on cancer.

A range of dynamic models[24] have been presented by many researchers to study natural occurrences so as to give a more worthwhile approach with better credibility. Fractional Calculus (FC) generalizes classical calculus by focusing on integration and differentiation of non-integer (fractional) orders. Fractional Calculus (FC) is a generalization of classical calculus that deals with integration and differentiation of non-integer (fractional) orders. The idea of fractional operators emerged nearly concurrently with classical operators. The earliest known reference to this concept appears in the correspondence between G. W. Leibniz and the Marquis de L'Hôpital in 1695, where the notion of the semi-derivative was first discussed. Fractional Calculus[25] is a forthcoming and novel strategy when dealing with practical and everyday instances which is currently being applied in many fields of Physics[26], Bio-mathematics[27,28], fluid mechanics[29], Electrical engineering[30], Business and finance[31], and countless more extensive disciplines and sectors. Fractional derivatives and integration is an essential part of fractional calculus and has started been focused on since the last few years in almost all fields of science and engineering. Some recent works in fractional calculus include the study done by Kumawat et al.[32] in modeling of allelopathic stimulatory phytoplankton, Bhatia et al.[33] modeled covid-19 disease dynamics and Alsubaie et al.[34] presented a fractional model for influenza epidemology.

Homotopy perturbation method (HPM)[35–37] is well-known technique in solving differential equations since a while. However, He's method with different integral transforms is hybrid of HPM and different transforms like Laplace, Fourier, Aboodh, Laplace Carson, Mohand etc. are relatively newer concept which helps to approach more complex models in fractional and fuzzy domains[38–41]. The He-Laplace method effectively addresses fractional derivatives, especially in the Caputo sense, facilitating a more straightforward application of initial conditions that are more intuitively aligned with physical contexts. Additionally, this method offers a framework for demonstrating the convergence and stability of solutions. The He-Laplace method is distinguished by its effectiveness, ease of use, and versatility in addressing a broad range of fractional differential equations, making it a crucial resource for researchers in various fields. For instance, Agarwal et al. utilized caputo fractional derivative for generalized glucose supply model[42], Alqahtani et al.[43] put forward a fractional analysis of streptococcus suis infection in pig-human population and Belgaid et al.[44] studied how caputo-fractional derivatives can be applied to model covid-19 model. In the present work, cancer treatment model using immunotherapy is being analyzed in a fractional framework in Caputo sense. The Caputo type fractional derivative is gaining traction in cancer modeling because it effectively captures memory and hereditary effects in biological processes. This method enables more accurate representations of tumor growth dynamics and the interactions between cancer cells and effector cells in the body. The Caputo fractional derivative provides a solid framework for tackling initial value problems across various fields, improving the modeling of complex, memory-dependent systems while facilitating intuitive initial condition setups. Its versatility and relevance make it a valuable tool in both theoretical and practical applications. The main aspect of cancer treatment is taken to be immunotherapy which is scrutinized in detail by taking all the parameters such as immune cells death rate, tumor cells growth rate and many others by carefully examining the implications each has on the treatment model.

The current study aims to offer deeper insights into various aspects of immunotherapy and contribute to cancer treatment by providing fractional modeling of cancer treatment with more accurate and realistic results as compared to traditional integer-order models earlier worked on. Fractional modeling highlights the fact that cancer treatments tend to take longer time period than other treatments and therefore can only be studied by taking into account an adequate time period stretching over days and months. An extensive analysis on effector and tumor cells profiles are considered with respect to different factors involved in the treatment so as to strengthen the credibility of the work done. In this manuscript, a theoretical and simulation-based study has been performed to examine the effects of various parameters on the cancer tumor model. Randomly selected parametric values were used in the simulations to assess their impact on effector and tumor cell profiles. In rest of the manuscript, basic definitions are in Sect. 2, the model has been presented in Sect. 3, positivity and boundedness of the solution is discussed in Sect. 4 whereas convergence and stability of the He-Laplace algorithm is presented in Sect. 5. Furthermore, the proposed methodology is given in Sect. 6 followed by numerical

evaluation in Sect. 7. The results and detailed 2d, 3d and contour graphical work is presented in Sect. 8. Finally, the article is concluded followed by future recommendations for our work in Sect. 9.

Preliminaries

Definition 1 The **Caputo's time-fractional derivative** ${}^{C}\mathbb{D}_{t}^{\beta}$[45], for any function $\mathcal{T}(t)$ can be defined as:

$$ {}^{C}\mathbb{D}_{t}^{\beta}\mathcal{T}(t) = \frac{1}{\Gamma(\kappa-\beta)}\int_{0}^{t}(t-\xi)^{\kappa-\beta-1}\mathcal{T}^{(\kappa)}(\xi)d\xi, \qquad \kappa-1<\beta\leq\kappa. \tag{1}$$

Definition 2 The **Laplace transform** $\mathbb{L}$ **connected with Caputo's time-fractional derivative** ${}^{C}\mathbb{D}_{t}^{\beta}$[46] can be expressed as:

$$ \mathbb{L}\{{}^{C}\mathbb{D}_{t}^{\beta}\mathcal{T}(t)\} = s^{\beta}\mathbb{L}\{\mathcal{T}(t)\} - \sum_{n=0}^{\kappa-1}s^{\kappa-n-1}\mathcal{T}^{(n)}(0), \qquad \kappa-1<\beta\leq\kappa. \tag{2}$$

where β is the fractional order at any time 't' and $\kappa\in\mathbb{N}$.

Model formulation

This section primarily focuses on fractional modeling for cancer treatment and therapy. The under consideration fractional system representing cancer model using Immunotherapy[18], which majorly comprises of two different categories i.e., $\mathbb{E}(\mathbb{t})$ and $\mathbb{T}(\mathbb{t})$ at any specific time 't' which represents the number of Effector immune cells (the cells which fight cancer or in other words tumor-suppressive cells) and Cancer Tumor cells (tumor causing cells) respectively.

Consider the following system using Immunotherapy as:

$$ \frac{d^{\beta}\mathbb{E}}{dt^{\beta}} = \mathcal{S} + \frac{\rho\mathbb{E}\mathbb{T}}{\alpha+\mathbb{T}} - \mathcal{C}_{1}\mathbb{E}\mathbb{T} - \mathcal{D}_{1}\mathbb{E}, \tag{3}$$

$$ \frac{d^{\beta}\mathbb{T}}{dt^{\beta}} = r\mathbb{T}(1-b\mathbb{T}) - \mathcal{C}_{2}\mathbb{E}\mathbb{T}, \tag{4}$$

with

$$ \mathbb{E}(0) = 566666, \quad \mathbb{T}(0) = 3181775, \quad \text{and} \quad 0<\beta<1. \tag{5}$$

Table 1 provided below describes all the various parameters involved in the used model which will be further applied in our next sections to arrive at the conclusion of what impact any of these have on the overall cancer tumor profile.

Positiveness and boundness of solution

Mathematical model is effective when the system solution remains non-negative and the initial condition stays positive for all $t>0$. In this section, we establish the above notion theoretically.

Theorem 1 The Solutions of the model is Non-Negative or Positive for all $t>0$ and given initial conditions $\mathcal{R}(0)>0$ where $\mathcal{R}(t)=(\mathbb{E},\mathbb{T})$.

Proof Consider the Effector cells Equation of our Cancer Model given in Eq. (3) :

Parameters	Notation
Regular rate of flow of immune cells into tumor site	$\mathcal{S}$
Recruitment rate of immune cells	ρ
Death rate of immune cells due to malignant cells attachment	$\mathcal{C}_1$
Rate of immune cells killing fractional tumor cells	$\mathcal{C}_2$
Immune cells death rate	$\mathcal{D}_1$
Immune cell attraction coefficient	α
Logistic or Intrinsic growth rate	r
Carrying capacity reciprocal	b

Table 1. Nomenclature.

$$\begin{aligned}\frac{d^{\beta}\mathbb{E}}{dt^{\beta}} &= \mathcal{S} + \frac{\rho\mathbb{E}\mathbb{T}}{\alpha+\mathbb{T}} - \mathcal{C}_1\mathbb{E}\mathbb{T} - \mathcal{D}_1\mathbb{E} \\ \frac{d^{\beta}\mathbb{E}}{dt^{\beta}} &= \mathcal{S} + \left(\frac{\rho\mathbb{T}}{\alpha+\mathbb{T}} - \mathcal{C}_1\mathbb{T} - \mathcal{D}_1\right)\mathbb{E}\end{aligned} \tag{6}$$

Now we assume: $\mu_1(t) = \frac{\rho\mathbb{T}}{\alpha+\mathbb{T}} - \mathcal{C}_1\mathbb{T} - \mathcal{D}_1$ and $\mu_2(t) = \mathcal{S}$, then our above equation becomes:

$$\frac{d^{\beta}\mathbb{E}}{dt^{\beta}} = \mu_1(t)\mathbb{E} + \mu_2(t)$$

Further simplifying it becomes:

$$\frac{d^{\beta}\mathbb{E}}{dt^{\beta}} - \mu_1(t)\mathbb{E} = \mu_2(t) \tag{7}$$

By applying Integrating factor concept we arrive at:

$$\begin{aligned}\left(\frac{d^{\beta}\mathbb{E}}{dt^{\beta}} - \mu_1(t)\mathbb{E}\right)\exp(-\int \mu_1(t)dt) &= \mu_2(t)\exp(-\int \mu_1(t)dt) \\ \frac{d^{\beta}}{dt^{\beta}}\left(\mathbb{E}\exp(-\int \mu_1(t)dt)\right) &= \mu_2(t)\exp(-\int \mu_1(t)dt)\end{aligned}$$

Therefore,

$$\mathbb{E}\exp\left(-\int \mu_1(t)dt\right) = {}^{C}\mathcal{I}_t^{\beta}\left(\exp(-\int \mu_1(t)dt)\right)\mathcal{S} \tag{8}$$

where, ${}^{C}\mathcal{I}_t^{\beta}$ is the caputo fractional integral of order beta. By applying the definition of Caputo Fractional integration definition[47], the Solution of the above equation becomes:

$$\mathbb{E}(t) = \mathcal{S}\left(\frac{1}{\Gamma(\beta)}\int_0^t \exp(t-\tau)^{\beta-1}f(\tau)d\tau\right)\left(\exp(-\int \mu_1(t)dt\right) > 0 \tag{9}$$

Similarly, it can easily be shown that $\mathbb{T}(t)$ is also positive for all time $t > 0$. □

Proposition 2 The solution $(\mathbb{E},\mathbb{T})$is bounded in the interval $[0,\infty)$, with $\lim_{t\to\infty} sup\mathcal{R}(t) \leq \mathcal{W}$ where $\mathcal{W}$ is disease free equilibrium point and $\mathcal{R}(t) = \mathbb{E}(t) + \mathbb{T}(t)$ then the solution $(\mathbb{E}, \mathbb{T})$ is bounded in the interval $[0, \mathbb{T})$ for every $t \in [0,\infty)$.[48]

Convergence and stability of He-Laplace algorithm

Theorem 3 For any two functions $\mathbb{E}_m(t)$ and $\mathbb{E}(t)$ defined within a Banach space, the approximate solution of the fractional model approaches its exact solution, with the constant $\mathbb{C}$ is confined to the interval $(0, 1)$.

Proof Consider the sequence of partial sums $\{\mathbb{S}_m\}$. We need to demonstrate that $\mathcal{S}_m$ forms a Cauchy sequence in the Banach space. For this purpose, let us examine:

$$\begin{aligned}\|\mathcal{S}_{m+1} - \mathcal{S}_m\| &= \|\mathbb{E}_{m+1}\| \\ &\leq \mathbb{C}\|\mathbb{E}_m\| \\ &\leq \mathbb{C}^2\|\mathbb{E}_{m-1}\| \\ &\vdots \\ &\leq \mathbb{C}^{m+1}\|\mathbb{E}_0\|,\end{aligned} \tag{10}$$

where, for the partial sums $\mathbb{S}_m$ and $\mathbb{S}_n$ with $m \geq n$ and $m, n \in \mathbb{N}$, applying the triangle inequality results in:

$$\begin{aligned}\|\mathbb{S}_m - \mathbb{S}_n\| &= \|(\mathbb{S}_m - \mathbb{S}_{m-1}) + (\mathbb{S}_{m-1} - \mathbb{S}_{m-2}) + \cdots + (\mathbb{S}_{n+1} - \mathbb{S}_n)\| \\ &\leq \|\mathbb{S}_m - \mathbb{S}_{m-1}\| + \|\mathbb{S}_{m-1} - \mathbb{S}_{m-2}\| + \cdots + \|\mathbb{S}_{m+1} - \mathbb{S}_m)\|.\end{aligned} \tag{11}$$

After substituting (10) in (11) we get:

$$\begin{aligned}\|\mathbb{S}_m - \mathbb{S}_n\| &\leq \mathbb{C}^m\|\mathbb{E}_0\| + \mathbb{C}^{m-1}\|\mathbb{E}_0\|\| + \cdots + \mathbb{C}^{m+1}\|\mathbb{E}_0\| \\ &\leq (\mathbb{C}^m + \mathbb{C}^{m-1} + \cdots + \mathbb{C}^{m+1})\|\mathbb{E}_0\| \\ &\leq \mathbb{C}^{m+1}(\mathbb{C}^{m-n-1} + \mathbb{C}^{m-n-2} + \cdots + \mathbb{C} + 1)\|\mathbb{E}_0\| \\ &\leq \mathbb{C}^{m+1}\left(\frac{1-\mathbb{C}^{m-n}}{1-\mathbb{C}}\right)\|\mathbb{E}_0\|.\end{aligned} \tag{12}$$

As we know that, $0 < \mathbb{C} < 1$, thus it gives $1 - \mathbb{C}^{m-n} < 1$. Consequently,

$$\|\mathbb{S}_m - \mathbb{S}_n\| \leq \frac{\mathbb{C}^{m+1}}{1-\mathbb{C}} \max|\mathbb{E}_0|. \tag{13}$$

Since, $\mathbb{E}_0$ is already bounded therefore,

$$\lim_{m,n\to\infty} \|\mathbb{S}_m - \mathbb{S}_n\| = 0. \tag{14}$$

Equation (14) demonstrates that $\mathbb{S}_m$ is a Cauchy sequence within a Banach space.

This property is significant because it confirms the convergence and stability of the He-Laplace algorithm. Specifically, the Cauchy criterion asserts that for any specified level of accuracy, there exists an index beyond which all terms of the sequence remain arbitrarily close to one another. As a result, this finding not only strengthens the mathematical foundation of the algorithm but also ensures that it will yield stable and consistent results as m approaches infinity. □

Proposed methodology

The proposed methodology for the solution and analysis in this study is He-Laplace algorithm which brings together an integration of Homotopy perturbation method along with Laplace transform in order to create a more efficient and effective way of tackling complex fractional systems. The Laplace definition of Caputo fractional derivatives is also applied on the Fractional part whereas the non-fractional part utilizes the traditional Laplace transform method.

Consider a highly non-linear, time fractional system of ordinary differential equations of the following form:

$$\begin{aligned}\mathbb{D}_t^\beta[\mathcal{T}(t)] + \mathcal{L}[\mathcal{T}(t)] + \mathcal{N}[\mathcal{T}(t)] - g_1(t) = 0, \\ \mathbb{D}_t^\beta[\mathcal{E}(t)] + \mathcal{L}[\mathcal{E}(t)] + \mathcal{N}[\mathcal{E}(t)] - g_2(t) = 0, \\ \kappa - 1 < \beta \leq \kappa, \quad t > 0,\end{aligned} \tag{15}$$

with

$$\begin{aligned}\mathcal{T}(t) = \xi_1, \\ \mathcal{E}(t) = \xi_2,\end{aligned} \tag{16}$$

where the unknown functions $\mathcal{T}(t)$ and $\mathcal{E}(t)$ are depending on time only and the time fractional derivative here is $\mathbb{D}_t^\beta$ and $g_1(t)$, $g_2(t)$ are the known functions. The fractional parameter is β and $\mathcal{L}$ and $\mathcal{N}$ here represent the linear and non linear operators respectively and ξ_1, ξ_2 are random constants in each equation.

The Algorithm begins by applying Laplace Transform $\mathbb{L}$ on (15) by which we obtain:

$$\begin{aligned}\mathbb{L}\{\mathbb{D}_t^\beta[\mathcal{T}(t)]\} + \mathbb{L}\{\mathcal{L}[\mathcal{T}(t)] + \mathcal{N}[\mathcal{T}(t)] - g_1(t)\} = 0, \\ \mathbb{L}\{\mathbb{D}_t^\beta[\mathcal{E}(t)]\} + \mathbb{L}\{\mathcal{L}[\mathcal{E}(t)] + \mathcal{N}[\mathcal{E}(t)] - g_2(t)\} = 0.\end{aligned} \tag{17}$$

By applying the fundamental definitions provided in Sect. 2, we can determine the Laplace transform of the fractional derivative. Definition 2 provides:

$$\begin{aligned}\mathbb{L}\{\mathcal{T}(t)\} - \left(\frac{1}{s^\beta}\right)\sum_{n=0}^{\kappa-1} s^{\kappa-n-1}\mathcal{T}^{(n)}(0) + \left(\frac{1}{s^\beta}\right)\mathbb{L}\{\mathcal{L}[\mathcal{T}(t)] + \mathcal{N}[\mathcal{T}(t)] - g_1(t)\} = 0, \\ \mathbb{L}\{\mathcal{E}(t)\} - \left(\frac{1}{s^\beta}\right)\sum_{n=0}^{\kappa-1} s^{\kappa-n-1}\mathcal{E}^{(n)}(0) + \left(\frac{1}{s^\beta}\right)\mathbb{L}\{\mathcal{L}[\mathcal{E}(t)] + \mathcal{N}[\mathcal{E}(t)] - g_2(t)\} = 0.\end{aligned} \tag{18}$$

The Homotopy of the system is:

$$\begin{aligned}\mathbb{H}_1 = (1-s)\left(\mathbb{L}\{\mathcal{T}(t)\} - \mathcal{T}_0(t)\right) + s\mathbb{L}\{\mathcal{T}(t)\} - s\left(\frac{1}{s^\beta}\right)\sum_{n=0}^{\kappa-1} s^{\kappa-n-1}\mathcal{T}^{(n)}(0) + s\left(\frac{1}{s^\beta}\right)\mathbb{L}\{\mathcal{L}[\mathcal{T}(t)] \\ + s\mathcal{N}[\mathcal{T}(t)] - sg_1(t)\},\end{aligned} \tag{19}$$

$$\mathbb{H}_2 = (1-s)\left(\mathbb{L}\{\mathcal{E}(t)\} - \mathcal{E}_0(t)\right) + s\mathbb{L}\{\mathcal{E}(t)\} - s\left(\frac{1}{s^\beta}\right)\sum_{n=0}^{\kappa-1} s^{\kappa-n-1}\mathcal{E}^{(n)}(0) + s\left(\frac{1}{s^\beta}\right)\mathbb{L}\{\mathcal{L} \quad [\mathcal{E}(t)] + s\mathcal{N}[\mathcal{E}(t)] - sg_2(t)\}, \tag{20}$$

where $\mathcal{T}_0(t)$ and $\mathcal{E}_0(t)$ are the initial guesses. By using Taylor series expansion of $\mathcal{T}(t)$ and $\mathcal{E}(t)$ with respect to s gives rise to:

$$\begin{aligned}\mathcal{T}(t) &= \mathcal{T}_0(t) + s^1\mathcal{T}_1(t) + s^2\mathcal{T}_2(t) + s^3\mathcal{T}_3(t) + s^4\mathcal{T}_4(t) + \ldots \\ \mathcal{E}(t) &= \mathcal{E}_0(t) + s^1\mathcal{E}_1(t) + s^2\mathcal{E}_2(t) + s^3\mathcal{E}_3(t) + s^4\mathcal{E}_4(t) + \ldots\end{aligned} \tag{21}$$

After substituting Eq. (21) in homotopy Eqs. (19) and (20) and comparing similar coefficients of s, we obtain the first order problems at s^1 as follows:

$$\begin{aligned}\mathbb{L}\{\mathcal{T}_1(t)\} + \mathcal{T}_0(t) - \left(\frac{1}{s^\beta}\right)\sum_{n=0}^{\kappa-1} s^{\kappa-n-1}\mathcal{T}^{(n)}(0) + \left(\frac{1}{s^\beta}\right)\mathbb{L}\{\mathcal{L}[\mathcal{T}_0(t)] + \mathcal{N}[\mathcal{T}_0(t)] - g_1(t)\} = 0, \\ \mathbb{L}\{\mathcal{E}_1(t)\} + \mathcal{E}_0(t) - \left(\frac{1}{s^\beta}\right)\sum_{n=0}^{\kappa-1} s^{\kappa-n-1}\mathcal{E}^{(n)}(0) + \left(\frac{1}{s^\beta}\right)\mathbb{L}\{\mathcal{L}[\mathcal{E}_0(t)] + \mathcal{N}[\mathcal{E}_0(t)] - g_2(t)\} = 0.\end{aligned} \tag{22}$$

Application of the Inverse Laplace transform leads to:

$$\begin{aligned}\mathcal{T}_1(t) + \mathbb{L}^{-1}\left\{\mathcal{T}_0(t) - \left(\frac{1}{s^\beta}\right)\sum_{n=0}^{\kappa-1} s^{\kappa-n-1}\mathcal{T}^{(n)}(0)\right\} + \mathbb{L}^{-1}\left\{\left(\frac{1}{s^\beta}\right)\mathbb{L}\{\mathcal{L}[\mathcal{T}_0(t)] + \mathcal{N}[\mathcal{T}_0(t)] - g_1(t)\}\right\} = 0, \\ \mathcal{E}_1(t) + \mathbb{L}^{-1}\left\{\mathcal{E}_0(t) - \left(\frac{1}{s^\beta}\right)\sum_{n=0}^{\kappa-1} s^{\kappa-n-1}\mathcal{E}^{(n)}(0)\right\} + \mathbb{L}^{-1}\left\{\left(\frac{1}{s^\beta}\right)\mathbb{L}\{\mathcal{L}[\mathcal{E}_0(t)] + \mathcal{N}[\mathcal{E}_0(t)] - g_2(t)\}\right\} = 0.\end{aligned} \tag{23}$$

Continuing in likewise manner, The k^{th} order problems at s^k is given by:

$$\begin{aligned}\mathbb{L}\{\mathcal{T}_k(t)\} + \left(\frac{1}{s^\beta}\right)\mathbb{L}\{\mathcal{L}[\mathcal{T}_{k-1}(t)] + \mathcal{N}[\mathcal{T}_{k-1}(t)]\} = 0, \\ \mathbb{L}\{\mathcal{E}_k(t)\} + \left(\frac{1}{s^\beta}\right)\mathbb{L}\{\mathcal{L}[\mathcal{E}_{k-1}(t)] + \mathcal{N}[\mathcal{E}_{k-1}(t)]\} = 0.\end{aligned} \tag{24}$$

Operating the Inverse Laplace Transform on above problems leads to k^{th} order solution accordingly.

$$\begin{aligned}\mathcal{T}_k(t) + \mathbb{L}^{-1}\left\{\left(\frac{1}{s^\beta}\right)\mathbb{L}\{\mathcal{L}[\mathcal{T}_{k-1}(t)] + \mathcal{N}[\mathcal{T}_{k-1}(t)]\}\right\} = 0, \\ \mathcal{E}_k(t) + \mathbb{L}^{-1}\left\{\left(\frac{1}{s^\beta}\right)\mathbb{L}\{\mathcal{L}[\mathcal{E}_{k-1}(t)] + \mathcal{N}[\mathcal{E}_{k-1}(t)]\}\right\} = 0.\end{aligned} \tag{25}$$

The approximate solution of the given general time-fractional ODE system is:

$$\begin{aligned}\mathcal{T}(t) &= \mathcal{T}_0(t) + \mathcal{T}_1(t) + \mathcal{T}_2(t) + \mathcal{T}_3(t) + \mathcal{T}_4(t) + \ldots \\ \mathcal{E}(t) &= \mathcal{E}_0(t) + \mathcal{E}_1(t) + \mathcal{E}_2(t) + \mathcal{E}_3(t) + \mathcal{E}_4(t) + \ldots\end{aligned} \tag{26}$$

In certain instances and under some conditions, we come across highly non-linear differential equations comprising of exponential, logarithmic, trigonometric and non-trigonometric terms which make it rather difficult to solve such problems using the readily available methods in literature. In such cases, He-Laplace tends to acquire series form solutions which are worthy alternatives to closed form solutions. A complete step by step procedure for the application of He-Laplace on any system of FDE will be provided in our next section.

Application of He-Laplace algorithm to fractional cancer model

When considering differential equations in a fractional framework, attaining an exact solution is mostly not possible, therefore comes the need to solve such complex fractional systems by using various kinds of numerical solutions. In the present work, He-Laplace technique has been applied to the above system of FDEs to solve the model equations and to make an articulate and logistical analysis.

Consider the cancer model as Eqs. (3) and (4) and applying Laplace Transform and also by utilizing definition 2, we have:

$$\begin{aligned}\mathbb{L}\{\mathbb{E}(t)\} - \left(\frac{1}{s}\right)566666 - \left(\frac{1}{s^\beta}\right)\mathbb{L}\left[\mathcal{S} + \frac{\rho\mathbb{E}\mathbb{T}}{\alpha+\mathbb{T}} - \mathcal{C}_1\mathbb{E}\mathbb{T} - \mathcal{D}_1\mathbb{E}\right] = 0, \\ \mathbb{L}\{\mathbb{T}(t)\} - \left(\frac{1}{s}\right)3181775 - \left(\frac{1}{s^\beta}\right)\mathbb{L}\left[r\mathbb{T}(1-b\mathbb{T}) - c_2\mathbb{E}\mathbb{T}\right] = 0.\end{aligned} \tag{27}$$

Now creating homotopies for our fractional system, we get

$$\begin{aligned}\mathbb{H}_1 &= (1-p)(\mathbb{L}\{\mathbb{E}(t)\} - \mathbb{E}_0(t)) + p\left(\mathbb{L}\{\mathbb{E}(t)\} - \left(\frac{1}{s}\right)566666 - \left(\frac{1}{s^\beta}\right)\mathbb{L}\left[\mathcal{S} + \frac{\rho\mathbb{E}\mathbb{T}}{\alpha+\mathbb{T}} - \mathcal{C}_1\mathbb{E}\mathbb{T} - \mathcal{D}_1\mathbb{E}\right]\right),\\ \mathbb{H}_2 &= (1-p)(\mathbb{L}\{\mathbb{T}(t)\} - \mathbb{T}_0(t)) + p\left(\mathbb{L}\{\mathbb{T}(t)\} - \left(\frac{1}{s}\right)3181775 - \left(\frac{1}{s^\beta}\right)\mathbb{L}\left[r\mathbb{T}(1-b\mathbb{T}) - c_2\mathbb{E}\mathbb{T}\right]\right).\end{aligned} \tag{28}$$

Further, by using the concept of Taylor series expansion, we arrive at the following form for both the Effector and Tumor cells as shown below:

$$\mathbb{E}(t) = \sum_{i=0}^{\infty} p^i \mathbb{E}_i, \tag{29}$$

$$\mathbb{T}(t) = \sum_{i=0}^{\infty} p^i \mathbb{T}_i, \tag{30}$$

where the conditions in 5 are used as the initial approximations or the zeroth order solution.

Now, by using Taylor series expansions from (29) and (30),we substitute them back into homotopy Eqs. (28) Now, comparing coefficients for different powers of '*p*', will subsequently produce various order problems or equations:

First order problem and solution

$$\begin{aligned}\mathbb{L}\{\mathbb{E}_1(t)\} + 566666 - \left(\frac{1}{s}\right)566666 - \left(\frac{1}{s^\beta}\right)\mathbb{L}\left[\mathcal{S} + \frac{\rho\mathbb{E}\mathbb{T}}{\alpha+\mathbb{T}} - \mathcal{C}_1\mathbb{E}\mathbb{T} - \mathcal{D}_1\mathbb{E}\right] = 0,\\ \mathbb{L}\{\mathbb{T}_1(t)\} + 3181775 - \left(\frac{1}{s}\right)3181775 - \left(\frac{1}{s^\beta}\right)\mathbb{L}\left[r\mathbb{T}(1-b\mathbb{T}) - c_2\mathbb{E}\mathbb{T}\right] = 0,\end{aligned}$$

with

$$\begin{aligned}\mathbb{E}_1(t) &= 0,\\ \mathbb{T}_1(t) &= 0.\end{aligned}$$

Applying Inverse Laplace transform gives rise to the following first order solution:

$$\begin{aligned}\mathbb{E}_1(t) &= -\frac{1}{\alpha^2\Gamma(\beta+1)}\left(1803003712150\alpha^2\mathcal{C}_1 t^\beta + 566666\alpha^2\mathcal{D}_1 t^\beta\right.\\ &\quad\left.+\alpha^2\left(-\mathcal{S}t^\beta - 1803003712150\alpha\rho t^\beta + 5736752136226066250\rho t^\beta\right)\right),\\ \mathbb{T}_1(t) &= -\frac{1}{\Gamma(\beta+1)}\left(-3181775\left(-(3181775b-1)rt^\beta - 566666c_2t^\beta\right)\right).\end{aligned} \tag{31}$$

Second order problem and solution

$$\begin{aligned}&\mathbb{L}\{\mathbb{E}_2(t)\} + \frac{1147350427245213250 0rs^{-1-2\beta}\rho}{\alpha^2} - \frac{365061090564813838851875 00brs^{-1-2\beta}\rho}{\alpha^2}\\ &\quad+\frac{10123692150625s^{-1-2\beta}\mathcal{S}\rho}{\alpha^2} - \frac{1803003712150rs^{-1-2\beta}\rho}{\alpha} - \frac{5736752136226066250brs^{-1-2\beta}\rho}{\alpha}\\ &\quad+\frac{3181775s^{-1-2\beta}\mathcal{S}\rho}{\alpha} - \frac{5807711257159302760564622890625 0s^{-1-2\beta}\rho^2}{\alpha^4}\\ &\quad+\frac{365061090564813838851875 00s^{-1-2\beta}\rho^2}{\alpha^3} - \frac{5736752136226066250s^{-1-2\beta}\rho^2}{\alpha^2} + 1803003712150rs^{-1-2\beta}\mathcal{C}_1\\ &\quad-5736752136226066250brs^{-1-2\beta}\mathcal{C}_1 + 3181775s^{-1-2\beta}S\mathcal{C}_1 - \frac{365061090564813838851875 00s^{-1-2\beta}\rho\mathcal{C}_1}{\alpha^2}\\ &\quad+\frac{1147350427245213250 0s^{-1-2\beta}\rho\mathcal{C}_1}{\alpha} - 5736752136226066250s^{-1-2\beta}\mathcal{C}_1^2\\ &\quad-\frac{650164477205336011524500 0s^{-1-2\beta}\rho\mathcal{C}_2}{\alpha^2} - 1021700901549191900s^{-1-2\beta}\mathcal{C}_1\mathcal{C}_2\frac{1021700901549191900s^{-1-2\beta}\rho\mathcal{C}_2}{\alpha}\\ &\quad+s^{-1-2\beta}S\mathcal{D}_1 - \frac{1147350427245213250 0s^{-1-2\beta}\rho\mathcal{D}_1}{\alpha^2} + \frac{3606007424300s^{-1-2\beta}\rho\mathcal{D}_1}{\alpha} - 3606007424300s^{-1-2\beta}\mathcal{C}_1\mathcal{D}_1\\ &\quad-566666s^{-1-2\beta}\mathcal{D}_1^2 = 0,\\ &\mathbb{L}\{\mathbb{T}_2(t)\} - 6442262118510971875 0b^2r^2s^{-2\beta-1} - 1721025640867819875 0b\mathcal{C}_2rs^{-2\beta-1}\\ &\quad+30371076451875br^2s^{-2\beta-1} - 1803003712150\mathcal{C}_2d_1s^{-2\beta-1} + 3606007424300\mathcal{C}_2rs^{-2\beta-1}\\ &\quad-\frac{1825305452824069194259375 0\mathcal{C}_2\rho s^{-2\beta-1}}{\alpha^2} + \frac{5736752136226066250\mathcal{C}_2\rho s^{-2\beta-1}}{\alpha}\\ &\quad-1021700901549191900\mathcal{C}_2^2s^{-2\beta-1} - 5736752136226066250\mathcal{C}_1\mathcal{C}_2s^{-2\beta-1}\\ &\quad+3181775\mathcal{C}_2\mathcal{S}s^{-2\beta-1} - 3181775r^2s^{-2\beta-1} = 0,\end{aligned}$$

with the following conditions:

$$\begin{aligned}\mathbb{E}_2(t) &= 0,\\ \mathbb{T}_2(t) &= 0.\end{aligned} \tag{32}$$

Again, applying Inverse Laplace Transform leads to the following second order solution:

$$\begin{aligned}\mathbb{E}_2(t) = &-\frac{1}{\alpha^4\Gamma(2\beta+1)}\Bigg[t^{2\beta}\Bigg(-5736752136226066250\alpha^2\rho^2+36506109056481383885187500\alpha\rho^2\\ &-3181775\alpha^2c_1\Bigg(-3606007424300\alpha\rho+1803003712150\alpha^2br+321110355556\alpha^2c_2+1133332\alpha^2d_1\\ &+11473504272452132500\rho-566666\alpha^2r-\alpha^2S\Bigg)+5736752136226066250\alpha^3b\rho r\\ &-36506109056481383885187500\alpha^2b\rho r-5736752136226066250\alpha^4c_1^2-566666\alpha^4d_1^2\\ &+10217009015491919000(\alpha-6363550)\alpha^2c_2\rho+3606007424300\alpha^3d_1\rho-11473504272452132500\alpha^2d_1\rho\\ &+\alpha^4d_1S-58077112571593027605646228906250\rho^2-1803003712150\alpha^3\rho r+11473504272452132500\alpha^2\rho r\\ &-3181775\alpha^3\rho S+10123692150625\alpha^2\rho S\Bigg)\Bigg],\\ \mathbb{T}_2(t) = &\frac{1}{\alpha^2\Gamma(2\beta+1)}\Bigg[3181775t^2\beta\Bigg(\alpha^2\left(20247384301250b^2-9545325b+1\right)r^2+c_2\{-1803003712150\alpha\rho\\ &+5409011136450\alpha^2br+1803003712150\alpha^2c_1+566666\alpha^2d_1+5736752136226066250\rho-1133332\alpha^2r-\alpha^2S\}\\ &+321110355556\alpha^2c_2^2\Bigg)\Bigg].\end{aligned}$$

Continuing in the same manner, higher-order problems and solutions can be attained.

$$\begin{aligned}\tilde{\mathbb{E}} &= \sum_{k=0}^{4}\mathbb{E}_k(t),\\ \tilde{\mathbb{T}} &= \sum_{k=0}^{4}\mathbb{T}_k(t).\end{aligned} \tag{33}$$

The final series form approximate solution of the above system of cancer-tumor model is given by Eq. (33) for both the Effector and Tumor cells respectively.

Results and discussion

The current manuscript presents a time-fractional cancer-tumor model using immunotherapy by applying He-Laplace Procedure. The major focus of this work is to discuss several kind of distinct parameters involved in the system of fractional equations and to figure out the effect of each on both the effector immune cells and the cancer-tumor cells one by one. The reason for this approach is due to the fact that cancer is very much still an enigma in the real world, still affecting and causing fatality to hundreds of thousands people everyday and by this detailed graphical analysis, we attempt to decipher and investigate which parameter causes the effector immune cells to grow drastically but in a constant stable manner while killing the tumor cells in the same conduct. Randomly selected parametric values were used in the simulations to assess their impact on effector and tumor cell profiles. These effects will assist in making decisions regarding treatment and future predictions.

Effect of fractional order 'β'

Initially, we begin by studying the effect of fractional order on the cancer-tumor model:

Figure 1 displays the effect of various fractional orders on model under consideration. With an increase in fractional order from $\beta = 0.7$ to $\beta = 0.8$, it can be seen that effector cells tend to increase while tumor cells tend to decrease. This shows that the fractional analysis of the model depicts an escalation or in other words, with the usage of immunotherapy on a cancer patient, the immune system is activated, which causes the immune cells to grow and simultaneously kills the cancer cells. Our immune system helps in both combating cancer cells and getting rid of defective cells within our bodies. Therefore, introduction of immunotherapy on a person will have an advantageous effect while combating the disease.

Effect of regular rate of flow of immune cells into tumor site $\mathcal{S}$

Further, we see the impact that the flow rate of immune cells into the site of cancer tumor has on the entire model as well. $\mathcal{S}$ is defined as the *regular rate of flow of the immune cells into the tumor site*.

Figure 2 shows the effect of the rate of flow of the immune cells into the tumor site on the model under examination. In this particular instance the value of β has been taken to be 0.9 to examine the exact impact that $\mathcal{S}$ has on the entire system. The values of $\mathcal{S}$ have been taken in an increasing order from $\mathcal{S} = 0.8 \times 10^4$

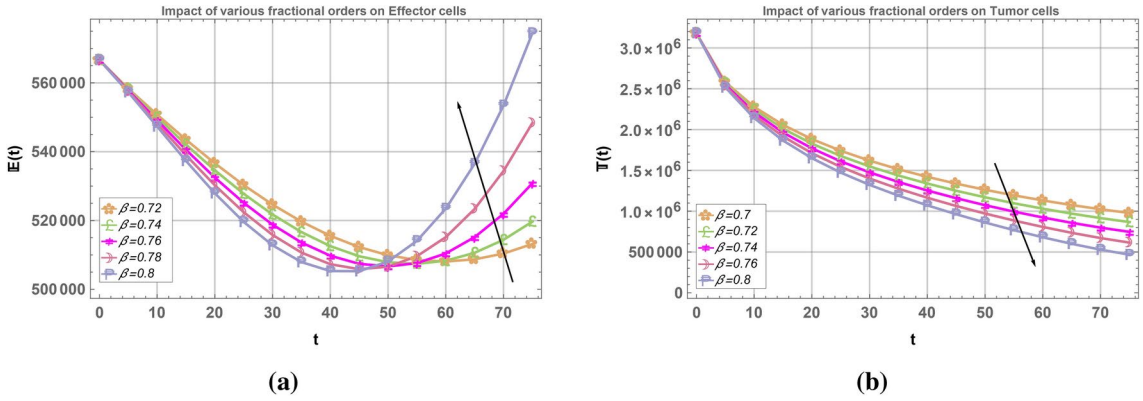

Fig. 1. Impact of different values of fractional order β.

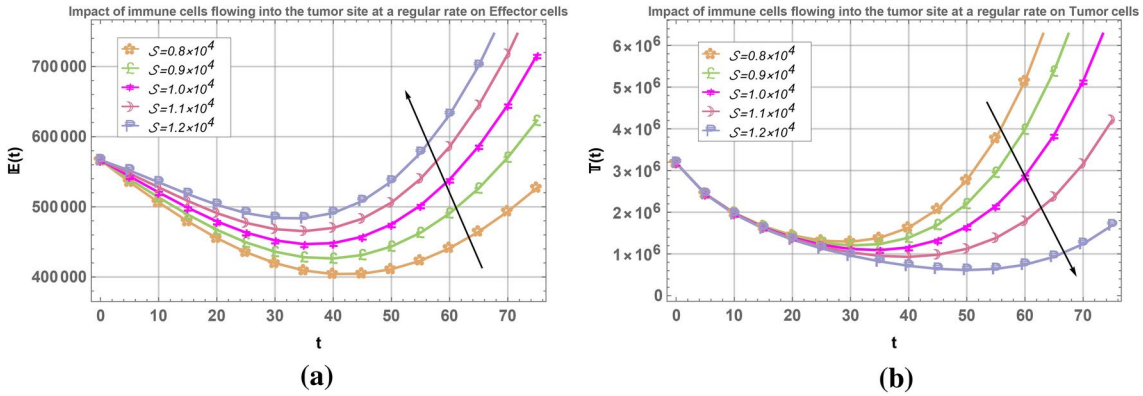

Fig. 2. Effect of Regular rate of flow of immune cells into tumor site $\mathcal{S}$ on Cancer Model while taking $\beta = 0.9$.

to $\mathcal{S} = 1.2 \times 10^4$, which depicts that we are increasing the flow rate of immune cells entering the tumor site at any time t. As soon as the flow is increased, there can be seen an increment of effector cellls and as synchronous decrease of tumor cells. The reason being that more amount of immune cells have been introduced into the body so the strength of a person's immune system has increased and consequently, it leads to the killing of tumor cells. On the account of the above behavior, it can be estimated that higher the flow rate of immune cells, the lesser the growth of tumor cells and the more the number of effector cells in the body.

Effect of recruitment rate of immune cells ρ

Advancing forward, the influence of the speed or intensity at which the immune cells progress towards the tumor site or towards any threat nearby on the entire model is put to test. $\boldsymbol{\rho}$ known as *recruitment rate of immune cells* refers to the highest speed or intensity at which immune cells are attracted to and move toward a site of infection, injury, or inflammation or the speed with which the immune system responds to a threat nearby. Figure 3 displays the effect of recruitment rate of immune cells on the cancer model. When discussing this outcome, the fractional order value is fixed to be $\beta = 0.8$ and the value of ρ is varied from $\rho = 0.12$ to $\rho = 0.14$. The profile then created shows that with an increase in the speed of immune cells being recruited, the effector cells are constantly increasing however with values nearer to the upper limit taken i.e $\rho = 0.14$, the increase is more as compared to the values near to the lower limit taken i.e $\rho = 0.12$. However, contrary to the effector cells beahvior, the tumor cells tend to be decreasing constantly but also in this case, the effect of decrement is more nearer to the upper limit i.e $\rho = 0.14$ than the lower limit i.e. $\rho = 0.12$. This displays that although increasing the speed does affect the overall profile of effector and tumor cells positively, i.e leads to more immune cells growth and kills more tumor cells, there needs to be an optimal value chosen for maximum benefit.

Effect of death rate of immune cells due to malignant cells attachment $\mathcal{C}_1$

Moving ahead, the result of death rate of immune cells due to their attachment with malignant cells or the cells which depict uncontrolled or unpredictable behavior is studied on our cancer model. $\mathcal{C}_1$ termed as *death rate of immune cells due to malignant cell attachment* refers to the proportion of immune cells that undergo programmed cell death or are otherwise rendered nonfunctional as a result of interacting with or being affected by cancerous (malignant) cells. Figure 4 illustrates the consequence of death rate of immune cells due to their attachment with cells having unclear behavior. In this case, the fractional order $\beta = 0.8$ is taken and the terms

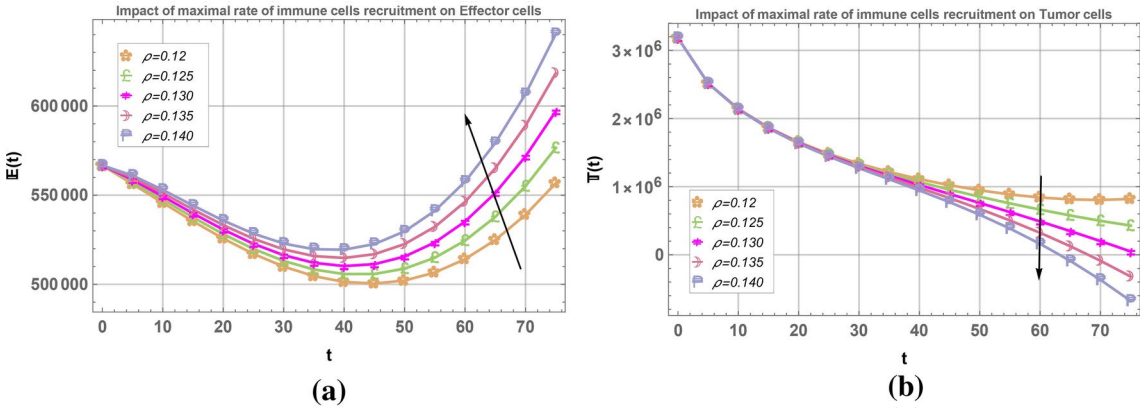

Fig. 3. Effect of recruitment rate of immune cells ρ on Cancer Model while taking $\beta = 0.8$.

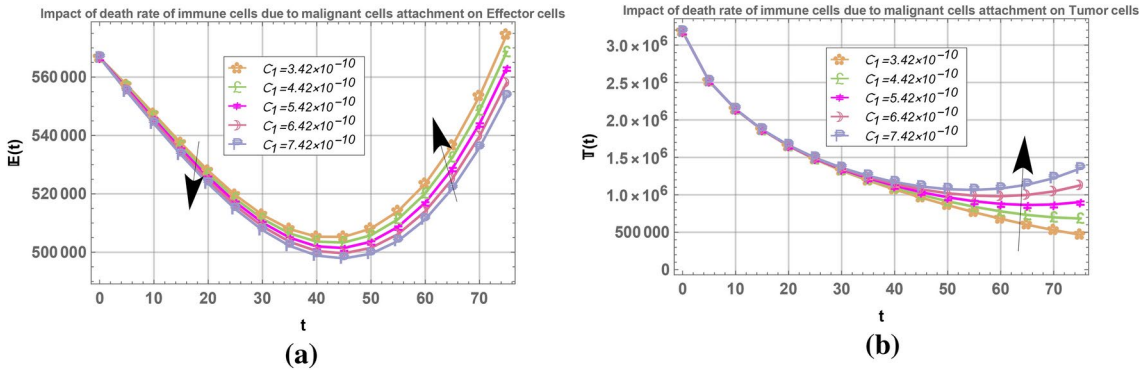

Fig. 4. Effect of recruitment rate of immune cells $\mathcal{C}_1$ on Cancer Model while taking $\beta = 0.8$.

of death rate are taken to be between $\mathcal{C}_1 = 3.42 \times 10^{-10}$ and $\mathcal{C}_1 = 7.42 \times 10^{-10}$. Whenever cancer treatment or even any other treatment is performed on an affected individual, it is not possible that only the tumor cells are treated in fact majority of the times other beneficial cells are also accidentally killed because any treatment cannot be focused only on one specified area of impact. For this reason, when the death rate of those immune cells which are *killed accidentally due to their attachment with malignant cells* rises up, the influence on effector cells also seems to be showing a behavior of decrement followed by increment. Particularly focusing on when $\mathcal{C}_1 = 3.42 \times 10^{-10}$, effector cells seem to be decreasing as immune cells death rate is rising up till when time is around 40 days but after 40 days have passed, the effector cells seem to be showing an increasing profile. The reason being that in the initial days, the body accidentally kills immune cells while targeting tumor cells but after a period of time, the effector cells decrease to a level that after that more tumor cells are being killed than effector cells and the immune cells quantity rises. The tumor cells, on the other hand, are decreasing drastically because in any case, the main motive of the treatment was to kill tumor cells. However, the lower limit taken i.e. $\mathcal{C}_1 = 3.42 \times 10^{-10}$ seems to be showing the most value of decrement in tumor cells and as the value increases to $\mathcal{C}_1 = 7.42 \times 10^{-10}$, lesser tumor cells are being targeted. Therfore, the value of death rate of immune cells due to their attachment with uncontrolled cells has a significant impact on the profile in general.

Effect of rate of immune cells killing fractional tumor cells $\mathcal{C}_2$

In this part, we study the impact that killing fractional tumor cells by immune cells has on the overall profile on the model under scrutiny. $\mathcal{C}_2$ represents the rate at which immune cells kill fractional tumor cells and b represents the *carrying capacity reciprocal* used to understand the effect that carrying capacity has on the tumor growth. Fractional tumor cells typically refer to a subset or proportion of tumor cells within a larger tumor or cancerous mass. These cells might be specifically targeted or studied in research to understand their behavior, treatment response, or role in the overall tumor dynamics. So, in this case, we are focusing on only a small portion of the tumor cells being targeted by immune cell to see the effect they have on the model. The fractional order is taken to be $\beta = 0.9$ and the value of $\mathcal{C}_2$ is varied from 1.1×10^{-7} to 5.1×10^{-7}. In Figure 5 it can be seen that, as the killing rate of a specified small portion of tumor cells rises, the overall effector cells profile also seems to be showing an increasing behavior. However, the Overall tumor profile does not have much impact on the smaller portion of tumor cells being killed, the reason is that the number of tumor cells killed might be very little as compared to the overall number of tumor cells present in the body. Consequently, although tumor cells

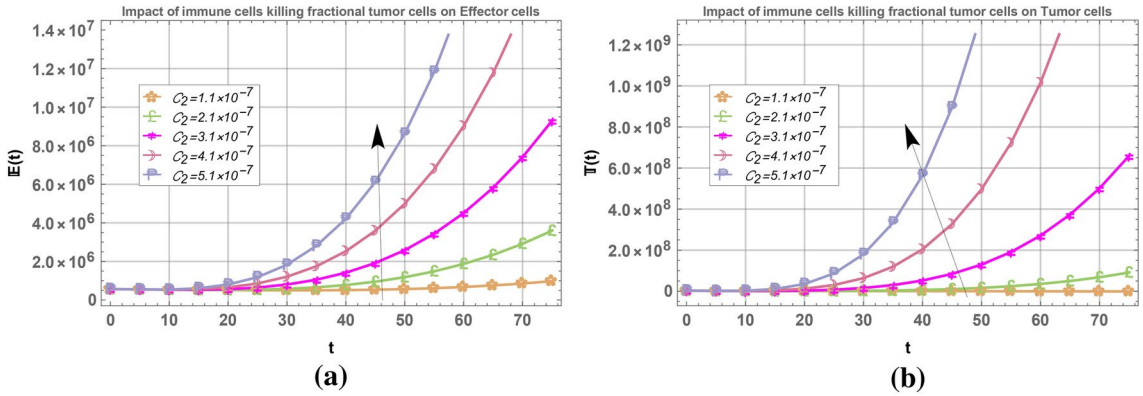

Fig. 5. Effect of killing rate of tumor cells by immune cells $\mathcal{C}_2$ on Cancer Model while taking $\beta = 0.9$.

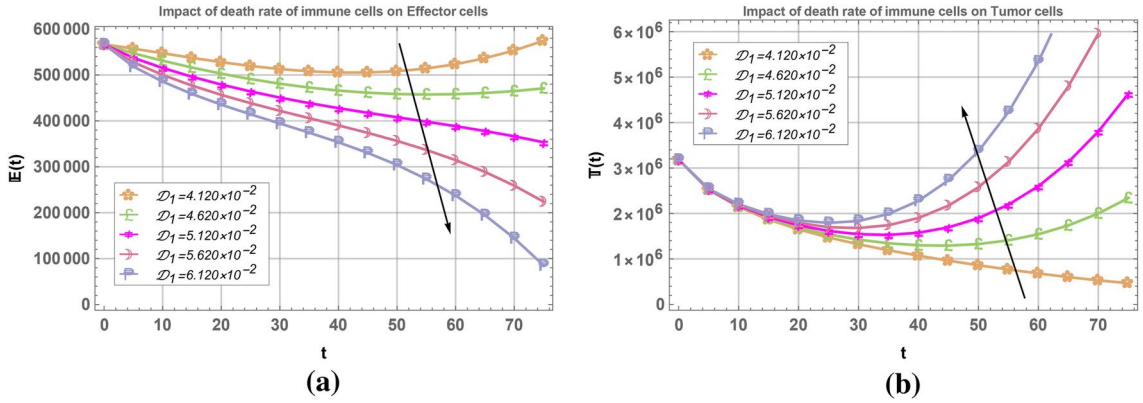

Fig. 6. Effect of killing rate of tumor cells by immune cells $\mathcal{D}_1$ on Cancer Model while taking $\beta = 0.8$.

are being killed, their effect is very little or negligible when viewed as bigger picture. Therefore, the impact of death rate of fractional cells by immune cells shows an interesting yet unpredictable behavior overall.

Effect of death rate of immune cells $\mathcal{D}_1$

In this portion, we try to figure out the impact that $\mathcal{D}_1$ death rate of immune cells tend to have on the cancer model as a whole. As is apparent from the name of the parameter under discussion, the death rate of immune cells should definitely mean that the effector profile should be declining, which can be illustrated in Fig. 6a. The fractional parameter was taken to 0.8 and the values of the death rate were varied from $\mathcal{D}_1 = 4.120 \times 10^{-2}$ to $\mathcal{D}_1 = 6.120 \times 10^{-2}$. The effector cells seems to be decreasing with all value of the death rate but as the death rate of immune cells has more impact when chosen $\mathcal{D}_1 = 6.120 \times 10^{-2}$ onward. Figure 6b shows that as the death rate of immune cells goes up, the tumor profile consequently goes down, as should have been the case. However, again when the value of death rate is taken around $\mathcal{D}_1 = 5.120 \times 10^{-2}$ onward, the tumor cells also rise up significantly as compared to the lower values. Therefore, the death rate of immune cells has a predictable behavior on the overall profile of cancer tumor we are dealing with.

Effect of immune cells attraction coefficient α

Given below is the effect of immune cells recruitment coefficient, which is a variable or parameter related to the rate or efficiency with which immune cells are recruited, taking into account the gradient or steepness of that process. An important function of innate immunity is the rapid recruitment of immune cells to sites of infection and inflammation through the production of cytokines and chemokines. α is defined as *immune cell attraction coefficient*, it is basically used to quantify how sharply or gradually immune cells are attracted to a specific location, it helps in determining the rate at which immune cells move towards the target area in response to signals such as cytokines. The process of recruiting immune cells by the immune system is very slow or negligible, the reason might be that cancer is a very complex disease, with an unpredictable behavior throughout so it initially becomes difficult for the immune system to fight it off immediately. This parameter tells us how quickly or effectively immune cells are recruited or attracted to a specific area. Figure 7a shows that the the speed with which immune cells are attracted to the target area is very slow which is why the effector cells seems to be declining with increasing values of α ranging from 2.020×10^7 to 6.020×10^7. The fractional parameter here is taken to be $\beta = 0.8$. Also, Fig. 7b depicts that with the increasing value of speed of immune cells the tumor

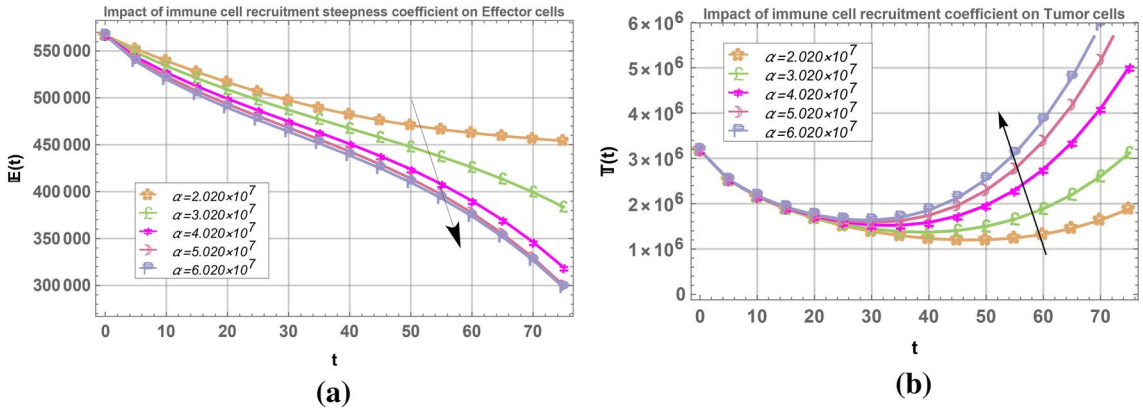

Fig. 7. Effect of Immune cells attraction coefficient α on Cancer Model while taking $\beta = 0.8$.

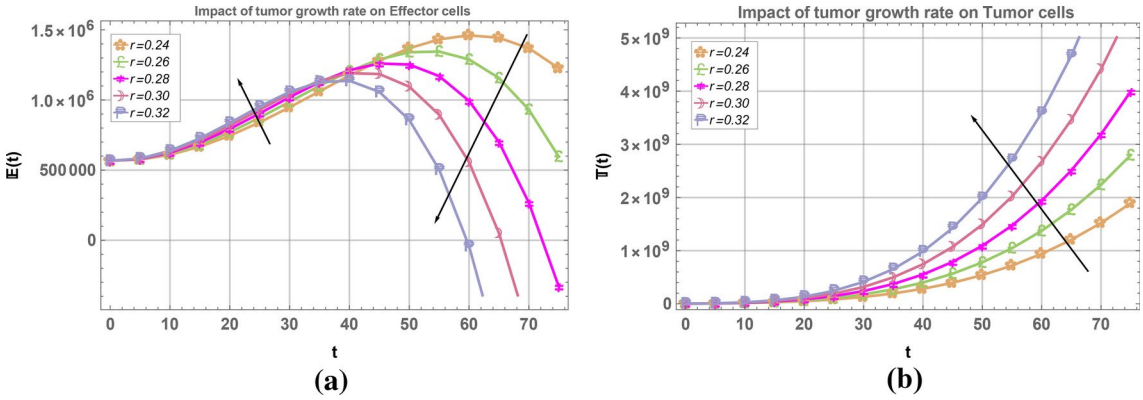

Fig. 8. Effect of Intrinsic growth rate *r* on Cancer Model while taking $\beta = 0.9$.

cells taking $\alpha = 2.020 \times 10^7$ initially do see some drastic decrease in tumor cells till around 45 days but after that the tumor cells irrespective of the speed of immune cells tend to be increasing. The reason might be that initially, the speed of immune cells were able to fight off tumor cells but with time the tumor cells start to grow stronger and greater in number that even with that speed, they are unable to eradicate the cancer cells. Another thing to be noted is that overall with the increase in speed, the tumor cells initially all show declining behavior but after some specific time, they all start to increase again, the highest α value having the most increasing behavior.

Effect of logistic/intrinsic growth rate *r*

The Intrinsic/Logistic growth rate is the parameter responsible for predicting the tumor cell growth population using the logistic model, its behavior on the cancer model is discussed in this part. It refers to the rate at which cell population grows under ideal conditions where resources are unlimited and environmental factors are constant. Therefore to sum it up, r is the *logistic/intrinsic growth rate* which predicts the growth of cell population under the logistic model. As the Logistic growth rate of cells is increasing, Fig. 8a depicts that at the outset, effector cells seem to be increasing at first for values of $r = 0.24$ to $r = 0.32$ after which for higher values of *r* the effector cells start to decline gradually. This shows the logistic behavior of growth i.e. the number of cells starts on increasing till it reaches a carrying capacity after which the cell count start to decline. The fractional order was assumed to be fixed at $\beta = 0.9$. Figure 8b shows the behavior which was expected i.e. the tumor growth rate keeps on increasing constantly as the parameter was one dependent on tumor growth rate.

Effect of carrying capacity reciprocal *b*

The parameter *b* is indicative of the carrying capacity of the growth that tumor undergoes. The carrying capacity reciprocal or inverse of tumor-bearing capacity would be a measure that reflects how much burden or impact the presence of a tumor places on the host or body. Figure 9a depicts that effector cells seem to be increasing till 40 days after which they reach the carrying capacity and start to decrease. The values of *b* are varied between 2.0×10^{-9} to 1.2×10^{-8} and fractional parameter is taken as 0.99. With increasing value of carrying capacity, effector cells seem to be decreasing. Figure 9b depicts that with increase in carrying capacity, tumor cells seem to be decreasing. This means that as the carrying capacity of the host body increases, tumor cells seem to be declining in size.

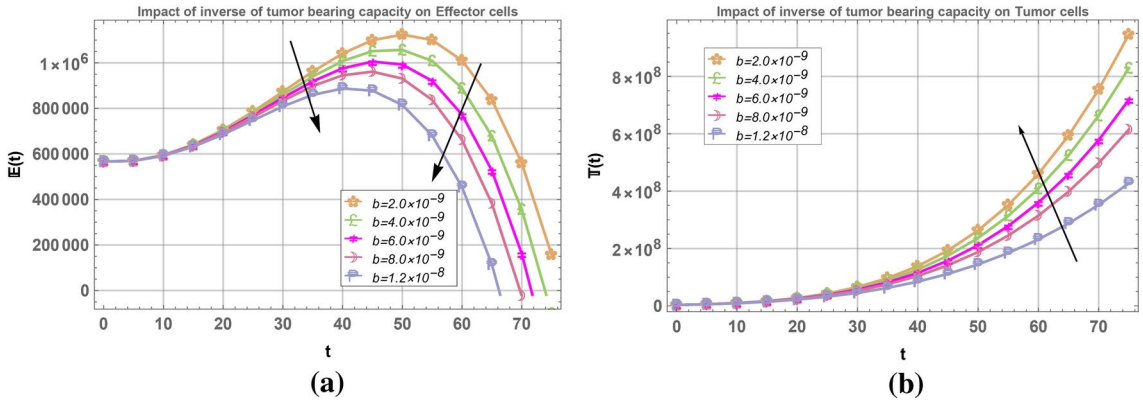

Fig. 9. Effect of Carrying Capacity Inverse b on Cancer Model while taking $\beta = 0.99$.

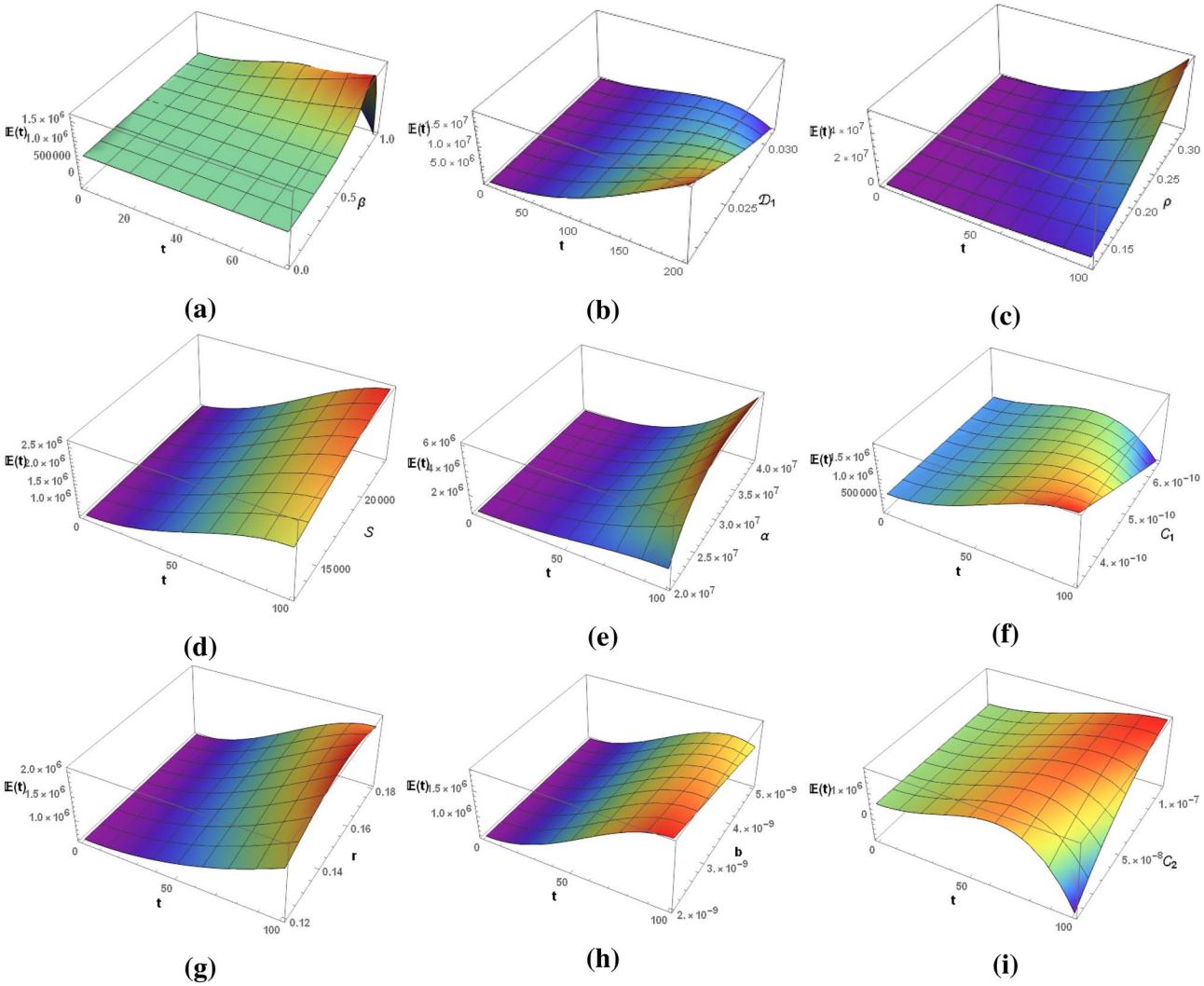

Fig. 10. 3D analysis of effector cells profile.

3D analysis of cancer model

Figure 10a depicts the 3D view of effector profile when plotted against the variable 't' time and the fractional parameter β. The fractional parameter is varied from 0 to 1, and time is also varied from 0 to 1. As time goes by, the effector cells seem to be increasing as time increases and the fractional order also increases. Similarly,

Fig. 11a depicts the tumor cells profile plotted against time 't' and fractional order β. It is seen that increase in time and β, tumor profile tends to be decreasing. Therefore, when this cancer model using immunotherapy is applied, effector immune cells will eventually increase and the cancer tumor cells will consequently decline in number.

Figure 10b shows the effect of death rate of immune cells from days t=0 to t=200 on effector cells while Fig. 11b depicts the same effect on tumor cells. As can be seen, as the death rate of immune cells rises, effector cells start to decline and on the other hand, tumor cells start to increase in number. Therefore, higher death rate of immune cells means higher tumor cells presence. Figure 10c depicts that recruitment rate of immune cells causes an increase in effector cells from t=0 to t=100 days and Fig. 11c alternatively shows the decrement of tumor cells in this case.

Figures 10d and 11d both display the behavior of effector and tumor cells within 100 days of treatment using our method with reference to Flow rate of immune cells within the site. The impact of Immune cells attraction coefficient is viewed in a 3D analysis in Figs. 10e and 11e where the patient's results are stimulated by considering a time interval of 100 days of therapy.

Death rate of immune cells having an effect on the effector and tumor profiles has been displayed in Fig. 10f and 11f during an interval of 100 days. Figs. 10g and 11g alongwith Figs. 10h and 11h represent the effect that logistic growth rate and carrying capacity respectively have on the effector and tumor quantity in the body side by side. The results of immune cells killing fractional tumor cells has been shown in Figs. 10i and 11i.

In all of the above Figs. from 10a to 11i displayed with the varying parameters in our cancer model, it can be seen that effector cells seem to be aligned with the paramters positively impacting immune cells whereas tumor cells seem to be decreasing with all parameters causing a decrease in cancerous cells in the body. This cancer model works most effectively when applied on a person when they are in the initial stages of cancer, since

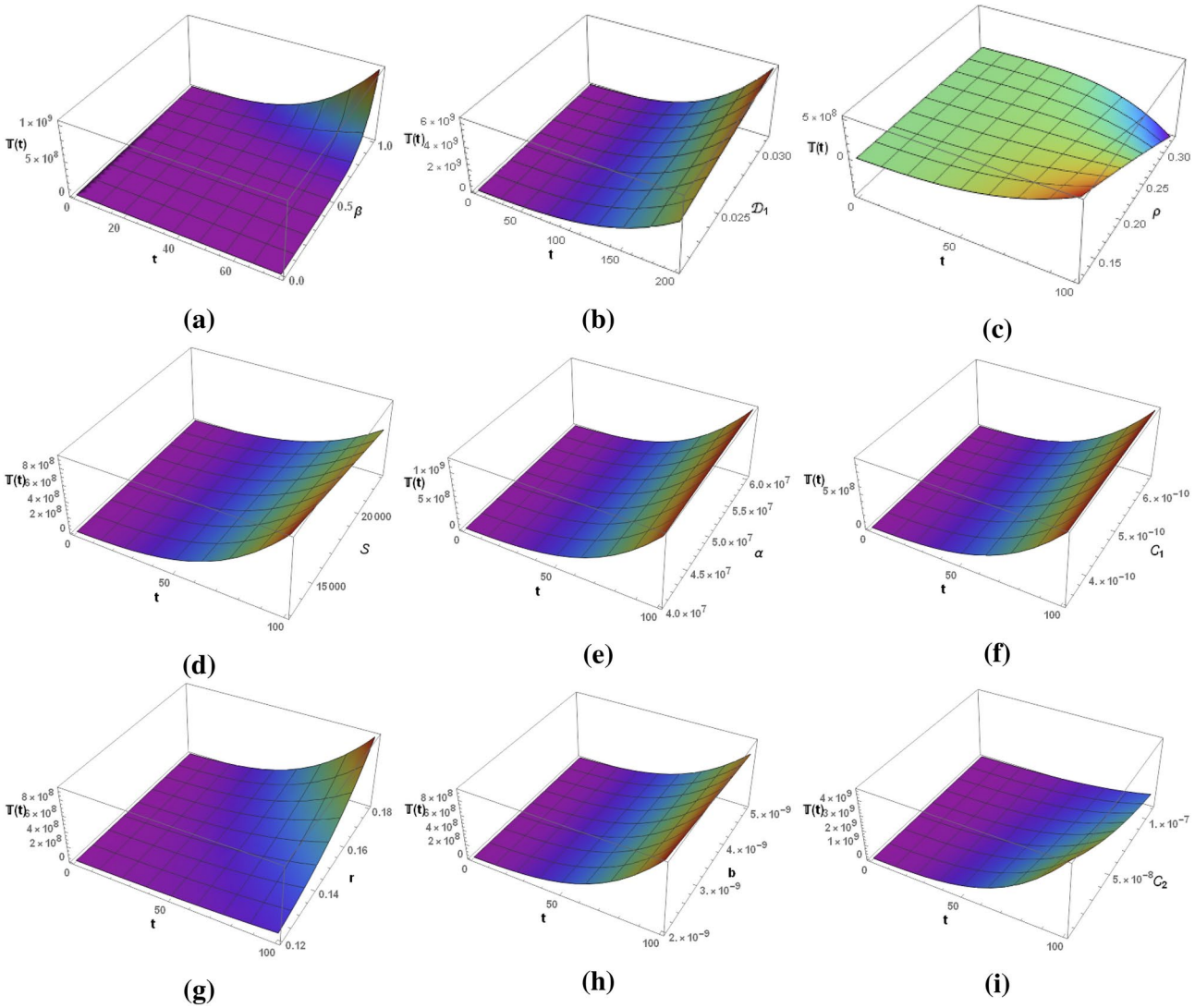

Fig. 11. 3D analysis of tumor cells profile.

immunotherapy is one of the initial treatments applied, where cancer is not too strong and this therapy can be applied so as to stop it from spreading to other body parts where more complex treatments would be required.

While we have optimized our current comprehensive numerical and graphical study to accurately represent the cancer treatment model, limitations, like those found in any numerical work, remain. The parameters utilized in the model may not account for all variations present in biological systems, because cancer as mentioned earlier is in itself yet a mystery to be solved. Therefore, our simulation based has, to the best of its ability, tried to capture this cancer model as efficiently as possible as explained and displayed in detail through our 2D and 3D plots, the findings of which in itself justify the study.

Contour analysis of cancer model

Contour graphs visually represent the spatial distribution and intensity of cancerous cells or tumors, helping to identify patterns and assess the effectiveness of the treatment, in the current work it tells whether the model under consideration using Immunotherapy is indeed effective or not. Figure 12a shows the contour plotting of Effector cells whereas Fig. 12b shows the contour plotting of Tumor cells. The fractional parameter is taken from 0 to 1 whereas the time duration is taken from $t = 0$ to $t = 75$. As can be clearly seen in the contours, as time 't' and β are increasing, so is the number of effector cells present whereas the tumor cells are decreasing in number. Therefore, it can be seen that fractional analysis of this cancer model depicts majority of the time an increase in immune cells and decrease in tumor cells, which is the ideal situation when the dealing with Cancer Tumor Models. Figure 13a depicts the contour model of Effector immune cells during the time from 0 to 75 days while varying the Logistics growth rate while Figure 13b shows the behavior of tumor cells on the same parameters. These results also show that effector cells increase proportionally and tumor cells decrease in the same manner. These results are valuable for medical practitioners in determining the scope of immunotherapy and its impact on tumor cells. Additionally, these findings allow medical professionals to validate the results in practical situations. This study paves the way for new approaches in cancer treatment.

Conclusion

The primary goal of this study was to develop a new solution for fractional cancer immunotherapy model using the He-Laplace procedure and to analyze the results. By applying a mixed algorithm of the Homotopy Perturbation Method (HPM) and the Laplace transform, we obtained a series solution for a nonlinear system of fractional differential equations (FDEs). We focused on two solutions: effector and tumor cell dynamics, evaluated through detailed graphical analysis across nine parameters. Our findings indicate that varying the fractional parameter β led to an increase in effector cells and a decrease in tumor cells, highlighting the effectiveness of the fractional approach. Increases in the rates of immune cell flow to the tumor site, recruitment rate of immune cells, and rate of immune cells killing fractional tumor cells correlated with rising effector counts and declining tumor numbers. Conversely, higher death rates of immune cells, carrying capacity parameters and logistic growth factors contributed to tumor growth and effector decline. Comprehensive 3D and contour analyses reinforced the model's effectiveness in depicting cancer-tumor interactions, supporting the notion that immunotherapy is a powerful treatment strategy. In future research, we aim to correlate our simulations with real data to enhance their relevance to real-world scenarios and deepen our understanding of cancer treatment complexities. Thus, our proposed method demonstrates strong potential for application to other nonlinear and complex systems in fields such as bio-mathematics, biotechnology, and biological engineering.

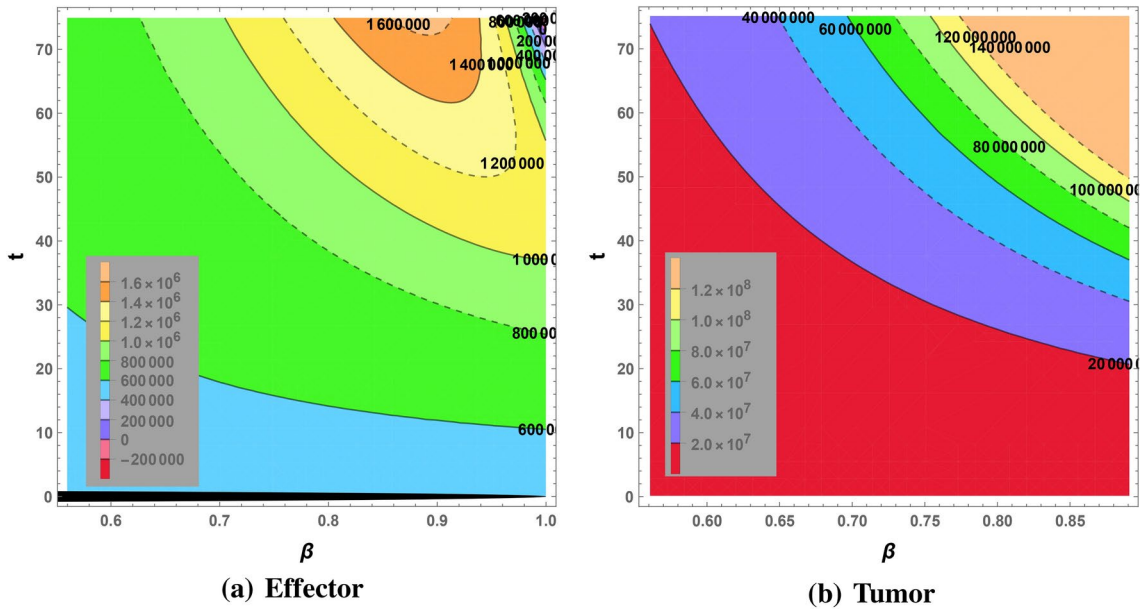

Fig. 12. Contour Analysis of cancer cells against fractional parameter.

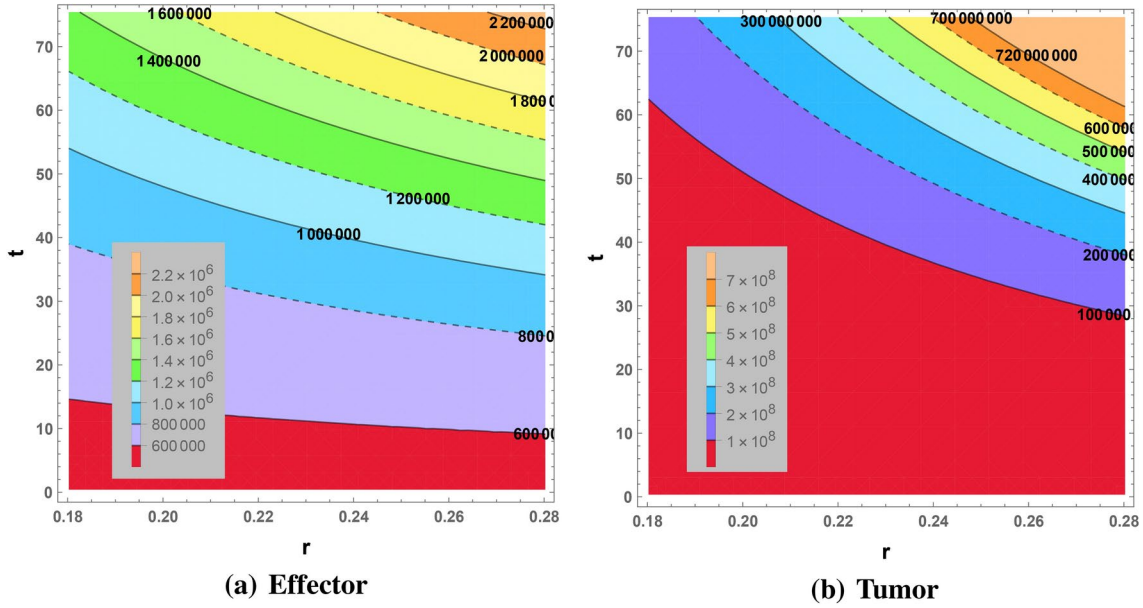

Fig. 13. Contour plotting of cancer cells against logistic growth rate.

Data availability

All data generated or analysed during this study are included in this published article.

Received: 5 September 2024; Accepted: 3 December 2024
Published online: 15 March 2025

References

1. Weinberg, R. A. How cancer arises. *Sci. Am.* **275**(3), 62–70 (1996).
2. Weinberg, R. A. & Weinberg, R. A. *The biology of cancer*. WW Norton & Company, (2006).
3. Qayyum, M. & Tahir, A. *Mathematical Modeling of Cancer Tumor Dynamics with Multiple Fuzzification Approaches in Fractional Environment* (Springer International Publishing, Cham, 2023).
4. Chanu, M. T. & Singh, A. S. Cancer disease and its' understanding from the ancient knowledge to the modern concept. *World J. Adv. Res. Rev.* **15**(2), 169–176 (2022).
5. Faguet, G. B. A brief history of cancer: Age-old milestones underlying our current knowledge database. *Int. J. Cancer* **136**(9), 2022–2036 (2015).
6. Smith, J. *Understanding What Cancer Is: Ancient Times to Present*. Health Press, (2023).
7. Pappalardo, F., Motta, S., Lollini, P-L. & Mastrian, E. Maths against cancer. In *More Progresses In Analysis*, pp 1351–1359. World Scientific, (2009).
8. Izadi, V., Farabad, E. & Azadbakht, L. Serum adiponectin level and different kinds of cancer: A review of recent evidence. *Int. Scholarly Res. Notices* **2012**(1), 982769 (2012).
9. Diez, P. J. G. R., Irma, H. & Russo, J. *The evolution of the use of mathematics in cancer research* (Springer Science & Business Media, Cham, 2012).
10. Butterfield, L.H., Kaufman, H.L. & Marincola, F.M. *Cancer immunotherapy principles and practice*. Springer Publishing Company, (2021).
11. Kirkwood, J. M. et al. Immunotherapy of cancer in 2012. *CA Cancer J. Clin.* **62**(5), 309–335 (2012).
12. Osotsi, J.I. *Mathematical modelling of the efficacy and toxicity of cancer chemotherapy*. PhD thesis, Strathmore University, (2017).
13. Enderling, H., Anderson, A. R. A., Chaplain, M. A. J., Munro, A. J. & Vaidya, J. S. Mathematical modelling of radiotherapy strategies for early breast cancer. *J. Theor. Biol.* **241**(1), 158–171 (2006).
14. Konstorum, A., Vella, A. T., Adler, A. J. & Laubenbacher, R. C. Addressing current challenges in cancer immunotherapy with mathematical and computational modelling. *J. R. Soc. Interface* **14**(131), 20170150 (2017).
15. Castiglione, F. & Piccoli, B. Cancer immunotherapy, mathematical modeling and optimal control. *J. Theor. Biol.* **247**(4), 723–732 (2007).
16. Bacaër, N & Bacaër, N.M. On epidemic modelling (1926–1927). *A short history of mathematical population dynamics*, pp 89–96, (2011).
17. Qayyum, M, Ahmad, E & Ali, M.R. New solutions of time-fractional cancer tumor models using modified he-laplace algorithm. *Heliyon*, 10(14), (2024).
18. Javeed, S, Ul A, Zain & Baleanu, D. Fractional modeling of cancer with mixed therapies. (2023).
19. Mathé, E. A. et al. Noninvasive urinary metabolomic profiling identifies diagnostic and prognostic markers in lung cancer. *Can. Res.* **74**(12), 3259–3270 (2014).
20. Zhang, X., Fang, Y., Zhao, Y. & Zheng, W. Mathematical modeling the pathway of human breast cancer. *Math. Biosci.* **253**, 25–29 (2014).
21. Quaranta, V., Weaver, A. M., Cummings, P. T. & Anderson, A. R. A. Mathematical modeling of cancer: The future of prognosis and treatment. *Clin. Chim. Acta* **357**(2), 173–179 (2005).
22. Tabassum, S, Rosli, N.B. & Binti M, Mazma S.A. Mathematical modeling of cancer growth process: a review. In *Journal of physics: conference series*, volume 1366, page 012018. IOP Publishing, (2019).
23. Lisette de Pillis, K. et al. Mathematical model creation for cancer chemo-immunotherapy. *Comput. Math. Methods Med.* **10**(3), 165–184 (2009).

24. Chaplain, M. A. J. & Lolas, G. Mathematical modelling of cancer invasion of tissue: Dynamic heterogeneity. *Netw. Heterogeneous Media* **1**(3), 399–439 (2006).
25. Hilfer, R. *Applications of fractional calculus in physics*. World scientific, (2000).
26. Qayyum, M, Ahmad, E, Alhefthi, RKS, Syed T & Inc, M. New solutions of time-fractional (3 + 1)-dimensional schrödinger model with multiple nonlinearities using hybrid approach in caputo sense. *Opt. Quantum Electr.*, 56(2), December (2023).
27. Magin, R, Fractional calculus in bioengineering, part 1. *Critical* Reviews ^{TM} *Biomed. Eng.*, 32(1), (2004).
28. Afzal, S., Qayyum, M., Riaz, M. B. & Wojciechowski, A. Modeling and simulation of blood flow under the influence of radioactive materials having slip with mhd and nonlinear mixed convection. *Alex. Eng. J.* **69**, 9–24 (2023).
29. Afzal, S, Qayyum, M & Chambashi, G. Heat and mass transfer with entropy optimization in hybrid nanofluid using heat source and velocity slip: a hamilton-crosser approach. *Sci. Rep.*, 13(1), July (2023).
30. Qayyum, M. & Ahmad, E. Fuzzy-fractional modeling and simulation of electric circuits using extended he-laplace-carson algorithm. *Phys. Scr.* **99**(6), 065020 (2024).
31. Qayyum, M., Ahmad, E., Tahir, A. & Acharya, S. Modeling and analysis of the fuzzy-fractional chaotic financial system using the extended he-mohand algorithm in a fuzzy-caputo sense. *Int. J. Intell. Syst.* **2023**, 1–15 (2023).
32. Kumawat, S., Bhatter, S., Bhatia, B., Purohit, S. D. & Suthar, D. L. Mathematical modeling of allelopathic stimulatory phytoplankton species using fractal-fractional derivatives. *Sci. Rep.* **14**(1), 20019 (2024).
33. Bhatter, S, Bhatia, B, Kumawat, S & Purohit, SD. Modeling and simulation of covid-19 disease dynamics via caputo fabrizio fractional derivative. *Comput. Methods Differ. Equ.*, (2024).
34. Alsubaie, N. E., Guma, F. E. L., Boulehmi, K., Al-kuleab, N. & Abdoon, M. A. Improving influenza epidemiological models under caputo fractional-order calculus. *Symmetry* **16**(7), 929 (2024).
35. He, J.-H. Homotopy perturbation technique. *Comput. Methods Appl. Mech. Eng.* **178**(3–4), 257–262 (1999).
36. He, J.-H. A coupling method of a homotopy technique and a perturbation technique for non-linear problems. *Int. J. Non-Linear Mech.* **35**(1), 37–43 (2000).
37. He, J.-H. Application of homotopy perturbation method to nonlinear wave equations. *Chaos, Solitons Fractals* **26**(3), 695–700 (2005).
38. Qayyum, M., Ahmad, E., Afzal, S. & Acharya, S. Soliton solutions of generalized third order time-fractional kdv models using extended he-laplace algorithm. *Complexity* **2022**(1), 2174806 (2022).
39. Qayyum, M., Ahmad, E., Akgül, A. & El Din, S. M. Fuzzy-fractional modeling of korteweg-de vries equations in gaussian-caputo sense: New solutions via extended he-mahgoub algorithm. *Ain Shams Eng. J.* **15**(4), 102623 (2024).
40. Qayyum, M. & Ahmad, E. New solutions of time- and space-fractional black-scholes european option pricing model via fractional extension of he-aboodh algorithm. *J. Math.* **2024**, 1–19 (2024).
41. Qayyum, M., Afzal, S., Ahmad, E., Akgül, A. & El Din, S. M. Generalized fractional model of heat transfer in uncertain hybrid nanofluid with entropy optimization in fuzzy-caputo sense. *Case Stud. Thermal Eng.* **55**, 104212 (2024).
42. Agarwal, H, Mishra, M.N. & Dubey, R.S. On fractional caputo operator for the generalized glucose supply model via incomplete aleph function. *Int. J. Math. Ind.*, 2450003, (2024).
43. Alqahtani, A. M. & Mishra, M. N. Mathematical analysis of streptococcus suis infection in pig-human population by riemann-liouville fractional operator. *Progr. Fract. Diff. Appl.* **10**, 119–35 (2024).
44. Belgaid, Y., Helal, M., Lakmeche, A. & Venturino, E. A mathematical study of a coronavirus model with the caputo fractional-order derivative. *Fractal Fract.* **5**(3), 87 (2021).
45. Abdel-Malek, H.L., Mohamed, A.S.A. & Ebid, S.E.K. On the fractional-order circuit design: Sensitivity and yield. In *Fractional Order Systems*, pp 271–304. Elsevier, (2018).
46. Vatsala, AS. & Sambandham, B. Laplace transform method for sequential caputo fractional differential equations. *Math. Eng., Sci. Aerospace (MESA)*, 7(2), (2016).
47. Castleberry, SK. *Understanding fractional integrals and their applications*. PhD thesis, Ph. D. dissertation, Georgia College and State University, (2018).
48. El Maroufy, H., Lahrouz, A. & Leach, P. G. L. Qualitative behaviour of a model of an sirs epidemic: Stability and permanence. *Appl. Math. Inf. Sci.* **5**(2), 220–238 (2011).

Author contributions

Writing a first draft: M.Q. and S.N.; Final Review: I.S. and A.G.; Supporting of materials reagent and data analysis tools: M.Q. and A.G.; Data analysis and interpretation: M.Q., S.N., I.S., and A.G.; Design experiments and supervision: M.Q.; Perform experiments: S.N.; Results validation: I.S.; All authors have read the final version of this manuscript and agreed to publish it.

Funding

This research did not receive any specific grant from funding agencies in the public, commercial, or not-for-profit sectors.

Declarations

Competing interests

The authors declare that they have no known competing financial interests or personal relationships that could have appeared to influence the work reported in this paper.

Additional information

Correspondence and requests for materials should be addressed to A.G.

Reprints and permissions information is available at www.nature.com/reprints.

Publisher's note Springer Nature remains neutral with regard to jurisdictional claims in published maps and institutional affiliations.

Open Access This article is licensed under a Creative Commons Attribution-NonCommercial-NoDerivatives 4.0 International License, which permits any non-commercial use, sharing, distribution and reproduction in any medium or format, as long as you give appropriate credit to the original author(s) and the source, provide a link to the Creative Commons licence, and indicate if you modified the licensed material. You do not have permission under this licence to share adapted material derived from this article or parts of it. The images or other third party material in this article are included in the article's Creative Commons licence, unless indicated otherwise in a credit line to the material. If material is not included in the article's Creative Commons licence and your intended use is not permitted by statutory regulation or exceeds the permitted use, you will need to obtain permission directly from the copyright holder. To view a copy of this licence, visit http://creativecommons.org/licenses/by-nc-nd/4.0/.

© The Author(s) 2025